Advanced Ceramics Progress: Vol. 11, No. 2, (Spring 2025) 50-59

Materials and Energy Research Center
MERC

Contents lists available at ACERP

Advanced Ceramics Progress

Journal Homepage: www.acerp.ir

Original Research Article

Optimizing Alumina Content in Leucite-Based Dental Glass-Ceramics: Crystallization, Microstructure, and Mechanical Properties

Mina Khosravi [a], Mahdi Kalantar [b]*

[a] *MS Student, Department of Mining and Metallurgical Engineering, Yazd University, Yazd, Iran.*
[b] *Professor, Department of Mining and Metallurgical Engineering, Yazd University, Yazd, Iran*

* Corresponding Author Email: mkalantar@yazd.ac.ir (M. kalantar) URL: https://www.acerp.ir/article_243081.html

ARTICLE INFO

Article History:
Received 25 November 2025
Received in revised form 23 December 2025
Accepted 06 February 2026

Keywords:
Leucite Glass-Ceramic,
Alumina,
Crystallization,
Heat Treatment,
Mechanical Properties

ABSTRACT

Leucite-based glass ceramics have attracted considerable attention in dental applications due to their optical similarity to natural dental tissues and their favorable mechanical properties. In this study, the influence of alumina content on the microstructure and physical, chemical, and mechanical properties of leucite glass ceramics was investigated. Starting materials containing 18–26 wt.% aluminum hydroxide, along with silica, sodium carbonate, potassium carbonate, and lithium carbonate, were homogenized, melted, and quenched to form glass frits. Compacted glass frit samples were subsequently heat treated and sintered at different temperatures ranging from 700 to 1000 °C. Thermal behavior, phase composition, and microstructure were evaluated using DTA, XRD, and SEM techniques, respectively. Physical and mechanical properties were characterized by measuring relative density, Vickers hardness, and flexural strength. The results indicated that the optimal heat-treatment temperatures for samples containing 18 wt.% and 22–26 wt.% aluminum hydroxide were 950 °C and 1000 °C, respectively. Increasing alumina content led to higher molten glass viscosity, delayed crystallization, and reduced sinterability of the glass frits. Consequently, alumina contents exceeding the stoichiometric amount resulted in decreased microstructural homogeneity, relative density, and mechanical properties.

https://doi.org/10.30501/acp.2026.562110.1188

1. INTRODUCTION

Ceramics such as porcelain, zirconia, and apatite-based compounds, glass-ceramics including mica-, lithium metasilicate or disilicate-, leucite-, Li–aluminosilicate-, and Mg–aluminosilicate-based systems, metal–ceramics consisting of dental alloys veneered with porcelain, and synthetic resin–glass ceramic composites are widely used as restorative dental materials due to their favorable aesthetic and mechanical characteristics (Aydınoğlu & Yoruç, 2017; Cattell et al., 2020; El-Meliegy & Van Noort, 2011; Fu, Engqvist, & Xia, 2020; Gómez Tamayo, Rueda Arango, & Ossa Henao, 2020; Höland & Beall, 2012; P. H. Kumar et al., 2015; Montazerian et al., 2023; Srichumpong et al., 2020; Zhang et al., 2014). Among these materials, glass-ceramics represent an advanced class of bioceramics produced through controlled in situ crystallization of a parent glass during a multi-stage heat treatment process. The heat-treatment parameters temperature, time, and heating or cooling rates, together with the presence of nucleating agents, play a critical role in controlling crystal size, volume fraction, and distribution, thereby governing the final properties of glass-ceramics (Höland & Beall, 2012; Srichumpong et al., 2020). Dental glass-ceramics must satisfy stringent clinical requirements, including high translucency, aesthetic appearance,

Please cite this article as: Khosravi, M. & Kalantar, M. (2025). Optimizing Alumina Content in Leucite-Based Dental Glass-Ceramics: Crystallization, Microstructure, and Mechanical Properties, *Advanced Ceramics Progress*, 11(2), 50-59. https://doi.org/10.30501/acp.2026.562110.1188

chemical durability, adequate strength, biocompatibility, wear resistance, and thermal properties comparable to those of natural teeth (Cattell et al., 2020; Montazerian et al., 2023).

Among the various dental glass-ceramics, leucite-based systems have attracted significant attention owing to their favorable combination of optical and mechanical properties. Leucite is a crystalline phase in the potassium aluminosilicate system $KAlSi_2O_6$, characterized by a relatively high coefficient of thermal expansion CTE, good mechanical properties, and excellent chemical stability (Kelly, Nishimura, & Campbell, 1996; Mackert Jr et al., 2001; Novembre, Gimeno, & Poe, 2019; Salimkhani et al., 2019; 橋本忍 et al., 2005). The high CTE of leucite enables effective thermal compatibility between porcelain veneers and metallic substructures, making leucite-based glass-ceramics particularly suitable for porcelain-fused-to-metal PFM restorations, inlays, veneers, and other restorative systems (Kelly, Nishimura, & Campbell, 1996; Mackert Jr et al., 2001; Novembre, Gimeno, & Poe, 2019; 橋本忍 et al., 2005).

Previous studies have demonstrated that the incorporation of leucite crystals into a glassy matrix enhances both the strength and fracture toughness of dental porcelains. Cattell et al (Zhang et al., 2008). reported a positive linear relationship between fracture toughness and leucite content in dental porcelains. Similarly, Morena et al (Yoon et al., 1994). showed that leucite-containing glass-ceramics exhibit significantly higher fracture toughness compared with leucite-free glasses. This improvement has been primarily attributed to crack deflection and crack-bridging mechanisms occurring around leucite particles or elongated leucite clusters (Chen et al., 2010; Yoon et al., 1994; Zhang et al., 2008). In addition to mechanical reinforcement, Kelly et al (Mrázová & Klouzkova, 2009). demonstrated that leucite crystals provide favorable light scattering and reflection behavior, resulting in surface textures and optical properties closely resembling those of natural teeth.

The physical and mechanical properties of leucite-based glass-ceramics can be further tailored through the addition of various modifiers and additives, including CaF_2, Na_2O, Li_2O, P_2O_5, LiF, MgO, CaO, ZrO_2, ZnO, TiO_2, B_2O_3, excess K_2O, and Al_2O_3 beyond stoichiometric compositions (Al-Sanabani, Madfa, & Al-Qudaimi, 2014; Baino & Verné, 2017; Chen et al., 2019; P. Kumar et al., 2015; Kumar et al., 2016; Stábile & Volzone, 2014; Sui, Yu, & Dong, 2011; Xie, Bell, & Kriven, 2010). These additives influence several key aspects of glass-ceramic processing and performance, such as reducing melting temperature, increasing melt flowability, modifying crystallization kinetics, suppressing the formation of undesired secondary phases for example kalsilite, and altering the microstructure through changes in leucite crystal size and distribution (Baino & Verné, 2017; Chen et al., 2010; Kumar et al., 2016; Sui, Yu, & Dong, 2011). However, contradictory results have been reported regarding the role of certain additives, particularly alumina, on sinterability and crystallization behavior, highlighting the need for systematic investigations.

Several synthesis routes have been employed for the fabrication of leucite and leucite-based glass-ceramics, including melting–quenching, sol–gel processing, and solid-state reactions. For instance, sol–gel-derived leucite powders with high purity have been synthesized at temperatures as low as 850 °C using CaF_2 as a modifier, which effectively suppressed kalsilite formation and reduced synthesis temperature (Denry & Kelly, 2008). In contrast, melting–quenching approaches have shown that variations in Na_2O/K_2O ratios can significantly affect melt viscosity and leucite crystallization behavior. Increasing Na_2O content up to a critical level enhances leucite crystallization; however, excessive Na_2O promotes kalsilite formation, which adversely affects both aesthetic and mechanical properties (Kelly, 2004). Furthermore, the addition of small amounts of Li_2O and Cs_2O has been reported to increase the thermal expansion coefficient of dental porcelains, improving compatibility with metallic substructures (Montazerian & Zanotto, 2017).

Despite extensive studies on leucite-based dental glass-ceramics, the specific role of alumina content on crystallization behavior, microstructural evolution, and the coupled physical–mechanical performance has not been systematically clarified. Previous works have primarily focused on the effects of alkali modifiers or fluorine-containing additives, while alumina has often been treated as a fixed or secondary component. In this study, alumina content is deliberately varied over a wide compositional range 18–26 wt.% $Al(OH)_3$ to elucidate its direct influence on crystallization kinetics, phase stability, sinterability, and mechanical properties. Furthermore, by correlating thermal analysis, phase evolution, microstructural features, and mechanical responses, this work provides a comprehensive structure–property relationship for leucite-based dental glass-ceramics. The results offer new insights for the compositional design and optimization of alumina-containing leucite glass-ceramics for dental restorative applications.

In this study, the effect of alumina content on the crystallization behavior, microstructural evolution, and mechanical performance of leucite-based dental glass-ceramics is systematically investigated. By focusing on alumina as a key compositional variable, this work aims to clarify its role in phase development and structure–property relationships, which has not been comprehensively addressed in previous studies. The findings provide new insights for the compositional design and optimization of leucite-based glass-ceramics for dental restorative applications.

2. MATERIALS AND METHODS

2.1. Materials

SiO_2 powder (99.6% purity) with an average particle size of 5 µm, K_2CO_3 powder (98.0% purity) with an average particle size of 3 µm, $Al(OH)_3$ powder (99.0% purity) with an average particle size of 6 µm, and Na_2CO_3 and Li_2CO_3 powders (99.0% purity) with an average particle size of 2 µm were used as raw materials. The compositions of the investigated glass samples (Table 1) were selected based on the stoichiometric composition of the leucite crystalline phase $KAlSi_2O_6$. The alumina content in the glass-ceramic samples was intentionally set either below or above the stoichiometric amount and was compensated by sodium and lithium oxides. The calculated precursor quantities corresponding to the final glass compositions are presented in Table 2.

TABLE 1. Composition of glass samples studied in this work

Sample coding	SiO_2	Al_2O_3	K_2O	Na_2O	Li_2O
A_{18} A_{18}	55.10	14.98	21.55	4.18	4.17
A_{22}	55.10	17.98	21.55	2.68	2.67
A_{26}	55.07	20.97	21.57	1.20	1.17

TABLE 2. Calculated precursor amounts based on the final glass composition in Table 1.

Sample coding	SiO_2	$Al(OH)_3$	K_2Co_3	Na_2Co_3	Li_2Co_3
A_{18}	43.33	18.03	24.88	8.13	5.63
A_{22}	43.84	22	25.22	5.28	3.66
A_{26}	44.41	26	25.56	2.37	1.66

2.2. Glass Powder Preparation

Leucite-based glass powders were prepared using the conventional melting–quenching route. Reagent-grade raw materials, including acid-washed SiO_2, $Al(OH)_3$, Na_2CO_3, K_2CO_3, and Li_2CO_3, were weighed according to the designed batch compositions. The mixtures were homogenized by ball milling for 4 h using zirconia balls to ensure chemical uniformity. The homogeneous mixture was then melted in a high-temperature laboratory furnace at 1600 °C with a heating rate of 10 °C/min and held at the peak temperature for 4 h. The molten glass was rapidly quenched in water to form glass frits, which were subsequently dried at 120 °C for 2 h and sieved to a particle size below 63 µm (−230 mesh). To evaluate the effect of particle size on DTA analysis, sample A18 was additionally sieved through a 30-mesh sieve, yielding a particle size of approximately 595 µm.

2.3 Fabrication of Glass-Ceramic Samples

Dense glass-ceramic samples were prepared through the heat treatment of pressed glass frit discs with a diameter of 10 mm at different temperatures (700–950 °C), using a heating rate of 10 °C/min and a holding time of 1 h.

2.4. Characterizations

The thermal behavior of glass frit samples A18, A22, and A26 was investigated using a DTA–TG device (STA 504, BAHR, Germany) at a heating rate of 10 °C/min in an air atmosphere, with an alumina crucible used as the reference. The phase composition of the glass-ceramic samples was determined by X-ray diffraction (D500, Siemens) operated at 30 mA and 40 kV using Cu Kα radiation. Phase identification was performed using X'Pert software.

The microstructure of the glass-ceramic samples, which were polished to 400–800 grit, etched with 2% hydrofluoric acid for 10 s, and gold-sputtered, was examined using a scanning electron microscope (Mira 3-XMU). The bulk density of all heat-treated samples was determined using the Archimedes method in accordance with ASTM C373-88. The relative density of the heat-treated A18, A22, and A26 samples was calculated based on the measured bulk density and the theoretical density of leucite. Hardness was evaluated using a Vickers hardness tester (MVK-H21, Akashi, Japan) under a load of 300 g with a dwell time of 15 s. The three-point flexural strength was measured on polished specimens with chamfered edges and dimensions of 20 × 3 × 3 mm, in accordance with ASTM C1161-13. Since leucite-based glass-ceramics are primarily used as dental restorative materials rather than load-bearing implants, flexural strength testing was selected as the most clinically relevant mechanical evaluation.

3. RESULTS AND DISCUSSION

3.1. Differential Thermal Analysis

According to the DTA curves of the glass frit samples (Figure 1: A18, A22, and A26), increasing the alumina content and decreasing the lithium and sodium contents from A18 to A26 result in an increase in the softening point of the glass frits.

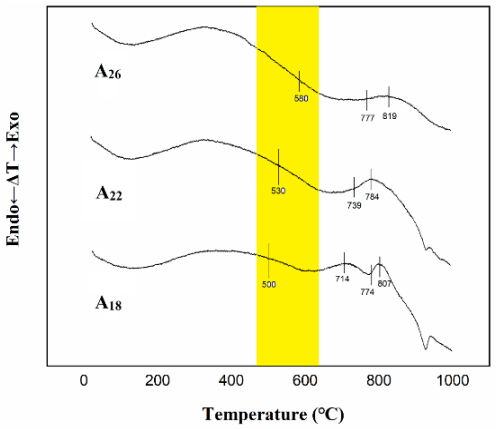

Figure 1. DTA curves for glass ferrite sample.

This effect is associated with a significant increase in the viscosity of the molten glass during melting for samples containing higher alumina contents. It should be noted that, in the glass industry, Na_2O is commonly added to reduce the melting temperature of silica-based glasses (Aydınoğlu & Yoruç, 2017).

The exothermic peaks observed in the DTA curves of all three samples correspond to the crystallization of glass phases. The first crystallization peak of sample A18 appears at a lower temperature (714 °C) compared with those of samples A22 and A26, which occur at 784 °C and 819 °C, respectively. This trend is consistent with reports indicating that Al_2O_3 increases network connectivity and raises the glass transition and crystallization temperatures (Tg/Tc) in silicate glasses by reducing the concentration and diffusivity of alkali cations (Gómez Tamayo, Rueda Arango, & Ossa Henao, 2020). In other words, increasing the alumina content while decreasing lithium and sodium contents delays glass crystallization and shifts it to higher temperatures. Reviews on dental glass-ceramics have also noted that compositions with higher alumina contents often require higher heat-treatment temperatures to achieve comparable crystallized fractions (P. H. Kumar et al., 2015).

Endothermic peaks observed at higher temperatures, around 900 °C, for samples with lower alumina contents (A18 and A22 in Figure 1) are associated with the transformation of secondary phases, such as kalsilite ($KAlSiO_4$), into leucite ($KAlSi_2O_6$), which is a diffusion-controlled process. For sample A18, which contains the lowest alumina content, this transformation appears as a more pronounced peak. With increasing alumina content, this peak gradually diminishes, and secondary phases tend to remain. As previously discussed, increasing Al_2O_3 content and reducing the concentration of alkali cations (lithium, sodium, and potassium) decrease ionic diffusivity, thereby hindering the transformation of kalsilite into leucite. Moreover, in the presence of higher Al_2O_3 contents, the kalsilite phase, which contains a higher proportion of alumina, is thermodynamically more stable than leucite. To investigate the effect of particle size, glass frit sample A18 with two different initial particle sizes of 0.063 mm and 0.595 mm was subjected to thermal analysis (Figure 2).

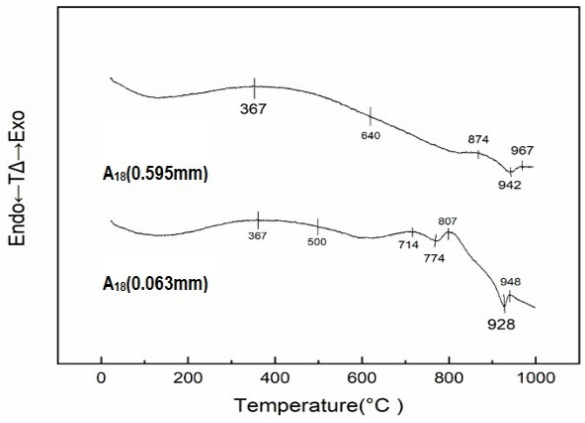

Figure 2. DTA of A18 with two different grain sizes

The crystallization peaks associated with the leucite phase for the fine-particle sample appear at lower temperatures and with higher intensity (807 °C compared with 874 °C for the coarse-particle sample). In addition, the average softening temperature of the fine-particle glass is approximately 500 °C, whereas that of the coarse-grained glass is about 640 °C. This behavior can be attributed to the higher specific surface area of the fine-particle sample, which enhances heat transfer and nucleation during thermal treatment.

3.2. Phase Composition

The X-ray diffraction patterns in Figure 3 reveal that the glass frit samples are fully amorphous. Upon heat treatment at temperatures ranging from 700 to 950 °C (Figs. 4a–e), pronounced crystallization occurs, and leucite emerges as the predominant crystalline phase in all investigated compositions.

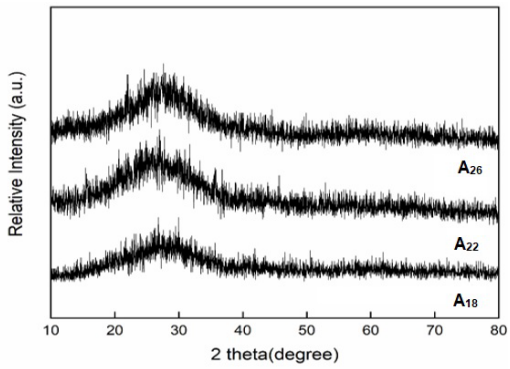

Figure 3. X-ray diffraction pattern of glass ferrite samples

In addition to the dominant leucite phase ($KAlSi_2O_6$, ICDD PDF No. 996-900-0486), secondary crystalline phases were detected in the XRD patterns, including potassium feldspar ($KAlSi_3O_8$, ICDD PDF No. 01-071-0911) in samples A18 (700–900 °C) and A22 (700–950 °C), and kalsilite ($KAlSiO_4$, ICDD PDF No. 00-012-0134) in sample A26 at higher temperatures (900–950 °C), as shown in Figure 4. These phases gradually disappeared at higher heat-treatment temperatures, such that at 950 °C for A18 and at 1000 °C for A22 and A26, the microstructure became dominated exclusively by the leucite phase (Figure 4e). This behavior is consistent with the thermodynamic stability of leucite at elevated temperatures compared with other potassium–aluminosilicate phases (Salimkhani et al., 2019).

Comparison of diffraction peak intensities at identical heat-treatment temperatures (Figure 4) reveals that the crystallization rate and growth of leucite crystals decrease with increasing alumina content. Alumina acts as a network former, increasing melt viscosity and restricting ionic diffusion, thereby delaying nucleation and crystallization of the glass phase (Al-Sanabani, Madfa, & Al-Qudaimi, 2014; Kelly, 2004; Montazerian & Zanotto, 2017). Accordingly, sample A26, which contains the highest alumina content, remains fully amorphous at 700 °C, and crystallization initiates only at temperatures of 900 °C and above.

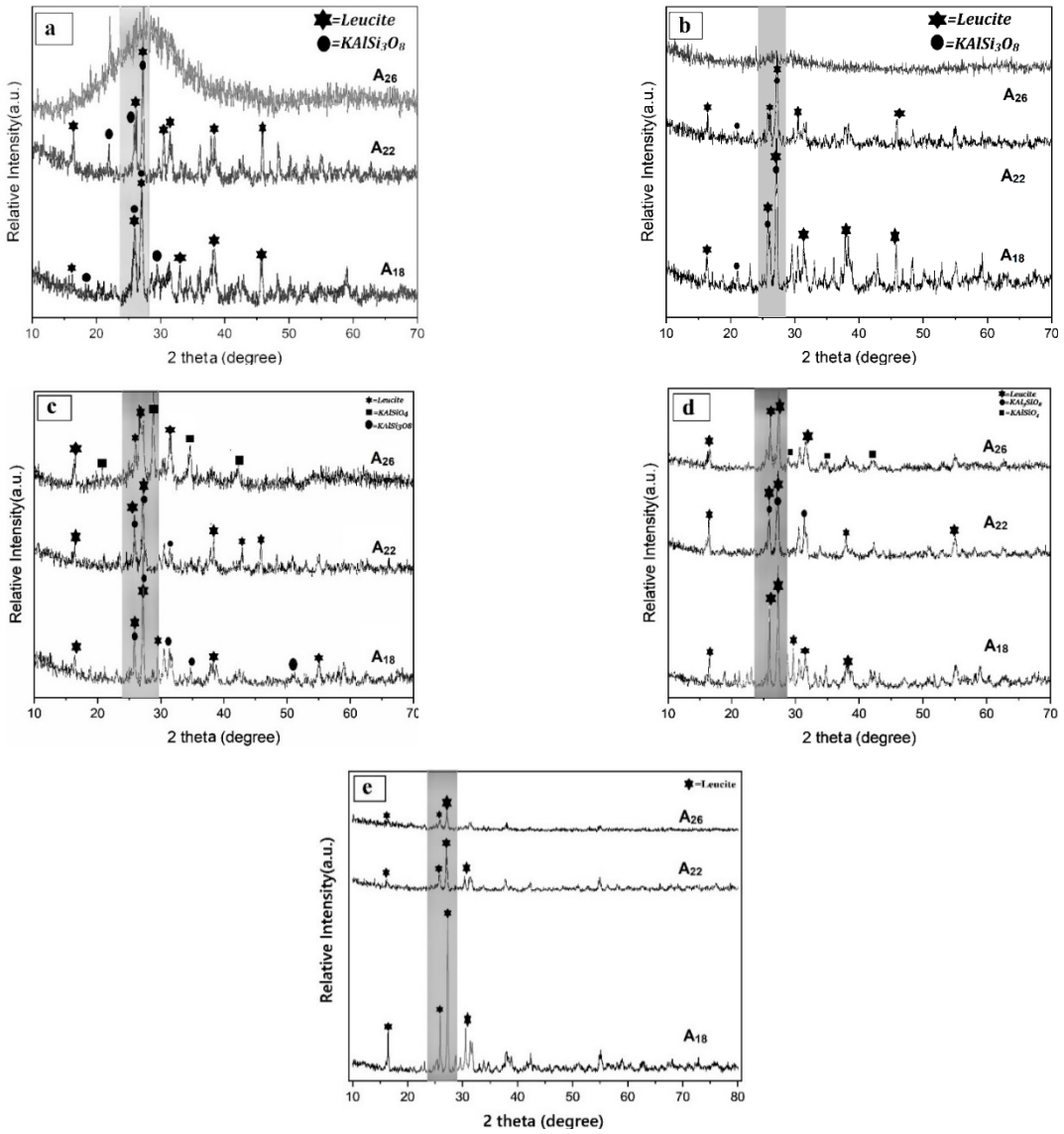

Figure 4. Phase composition of heat-treated samples at temperatures of a) 700, b) 800, c) 900, d) 950, and e) 1000°C

The presence of kalsilite and potassium-rich feldspar phases indicates incomplete phase transformation and diffusion-limited crystallization, particularly in alumina-rich compositions. These secondary phases, although present in limited amounts, can contribute to increased microstructural heterogeneity and residual porosity, adversely affecting densification and mechanical performance.

In contrast, samples with a higher volume fraction of leucite and minimal secondary phases exhibit improved microstructural homogeneity and superior mechanical properties. Based on these results, sufficient crystallization was achieved at 900, 950, and 1000 °C for heat-treated samples A18, A22, and A26, respectively. Therefore, microstructural and mechanical characterizations were conducted on samples treated at these optimized temperatures.

3.3. Relative Density

The variation in relative density with alumina content can be attributed to changes in glass viscosity and crystallization behavior. According to Table 3, the A18 samples exhibited higher relative density due to enhanced viscous flow sintering and earlier crystallization of the leucite phase. Similar behavior has been reported by Cattell et al. and Denry and Holloway, who demonstrated that lower alumina contents promote densification in leucite-based dental glass-ceramics by facilitating particle rearrangement and pore elimination during heat treatment (Denry & Holloway, 2010; Salimkhani et al., 2019). In contrast, increasing alumina content in A22 and A26 samples resulted in higher melt viscosity and delayed crystallization, which hindered densification and led to increased residual porosity. Comparable trends were reported by Siqueira et al. and

Montazerian and Zanotto, who showed that excessive alumina suppresses nucleation kinetics and reduces sinterability in aluminosilicate glass-ceramics (Kumar et al., 2016).

3.4. Microstructure

SEM micrographs of the heat-treated samples A18 at 900 °C, A22 at 950 °C, and A26 at 1000 °C are shown in Figs. 5–7, respectively. Sample A18 (Figure 5) exhibits a relatively homogeneous and dense microstructure with finer crystalline grains, which is consistent with the higher relative density measured for this composition. At higher magnifications (Figs. 5b and 5c), well-developed crystallized regions are clearly observable within the microstructure. As shown in Figs. 6 and 7, the degree of microstructural homogeneity in samples A22 and A26 is lower than that of A18. Sample A22 exhibits the highest porosity and microstructural heterogeneity, indicating the lowest sinterability among the three compositions. As discussed earlier, increasing alumina content delays leucite crystallization and requires higher heat-treatment temperatures to promote crystal formation. Consequently, more pronounced grain growth occurs, resulting in a more heterogeneous microstructure (Baino & Verné, 2017; Fu, Engqvist, & Xia, 2020; Zhang et al., 2014). Grain size analysis was performed using Digimizer software. The average grain sizes of the crystalline phases in samples A18, A22, and A26 were determined to be 2.78, 4.89, and 3.21 µm, respectively. The larger average grain sizes observed in A22 and A26 compared with A18 can be attributed to the higher heat-treatment temperatures and increased microstructural heterogeneity associated with higher alumina contents (Baino & Verné, 2017).

The smaller average grain size of A26 relative to A22 is likely due to the presence of potassium-rich feldspar phases in A22, which facilitate diffusion and promote enhanced grain growth of leucite crystals (Fu, Engqvist, & Xia, 2020). According to the EDX analysis of the heat-treated A22 sample (Figure 8), the elemental composition closely corresponds to the stoichiometric composition of leucite, with approximate atomic percentages of K: 10, Al: 10, Si: 20, and O: 60. The near-stoichiometric elemental ratios observed for leucite in sample A22 are consistent with the expected K–Al–Si compositions reported for dental leucite phases in the literature (Gómez Tamayo, Rueda Arango, & Ossa Henao, 2020).

TABLE 3. Properties of glass-ceramic samples, A_{18} heat treated at 900, A_{22} heat treated at 950 and A_{26} heat treated at1000℃

Glass-ceramic	Hardness Vickers	Relative density (%)	bending strength (MPa)
A18	673±20	94	49±2
A22	540±46	74	37 ± 8
A26	611±51	85	44± 9

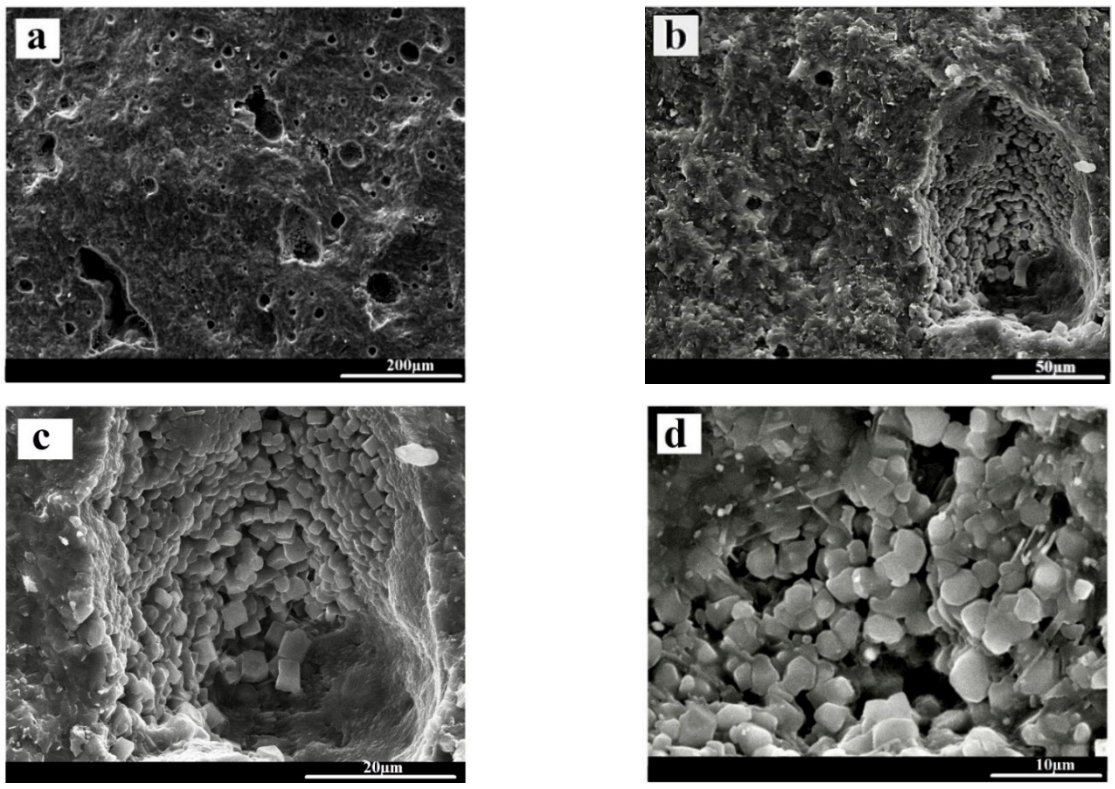

Figure 5. Microstructure of A18 after heat treatment at 900°C for 1 hour with different magnifications

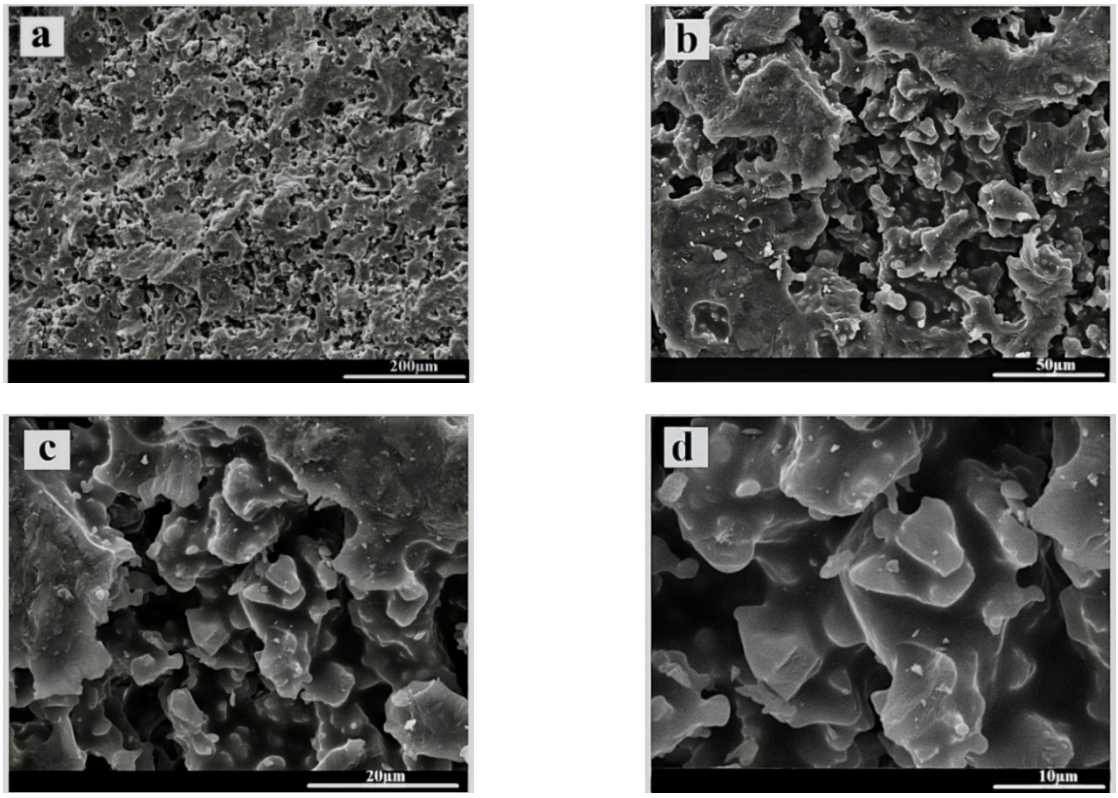

Figure 6. Microstructure of A22 after heat treatment at 950°C for 1 hour with different magnifications

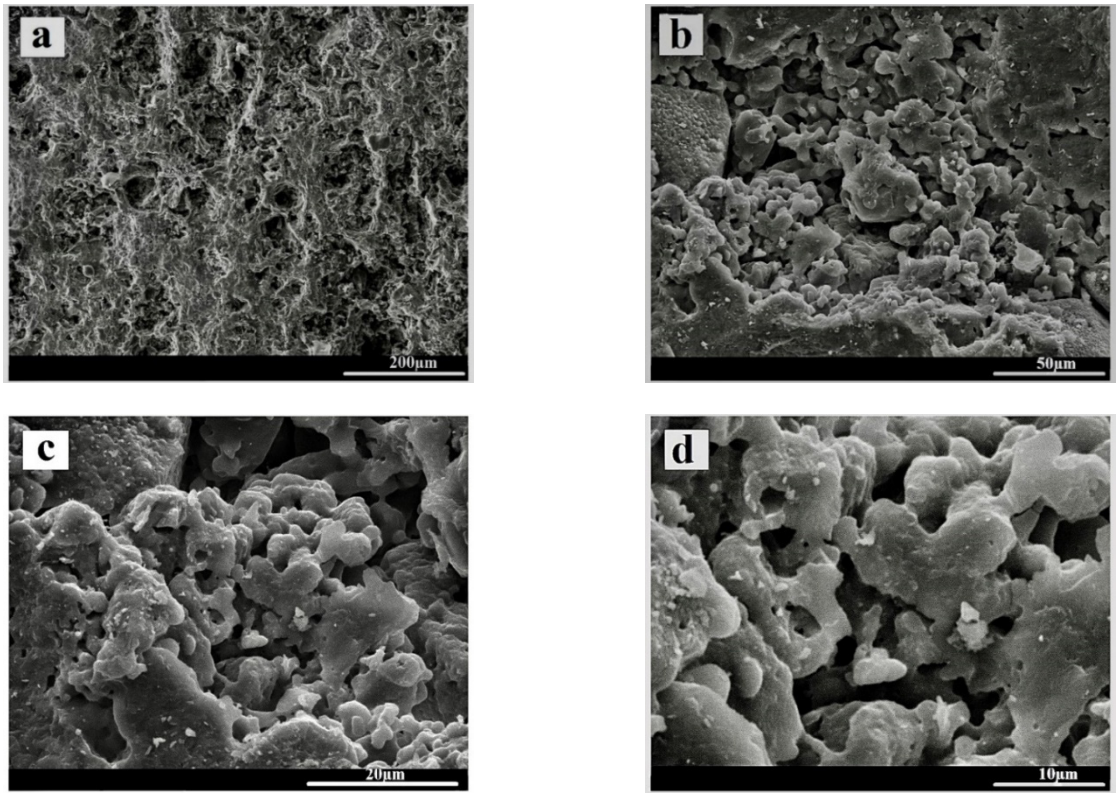

Figure 7. Microstructure of A26 after heat treatment at 1000°C for 1 hour with different magnifications

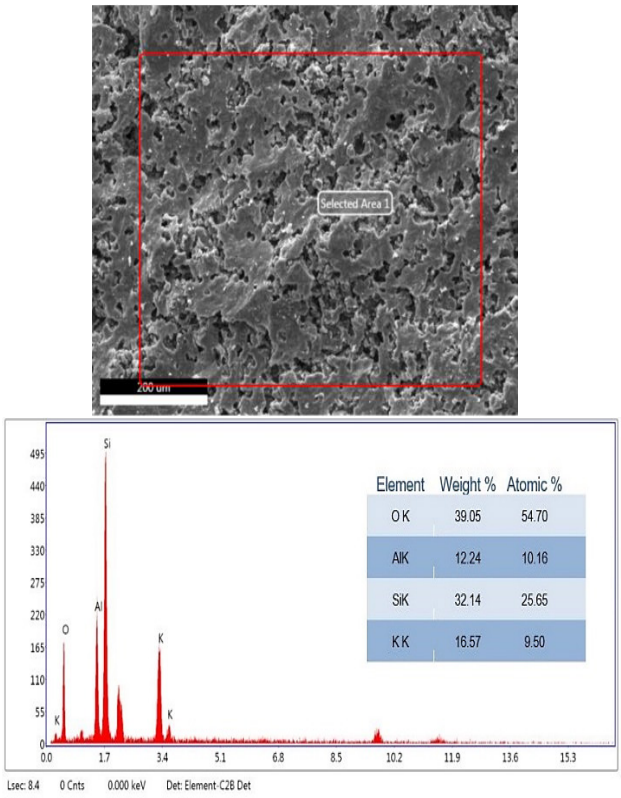

Figure 8. EDX of selected zone in microstructure of A22 heat treated at 950°C

The delay in leucite crystallization with increasing alumina content can be explained by kinetic and structural considerations. Alumina acts as a strong network former in silicate glasses, increasing network connectivity through the formation of Al–O–Si bonds and consequently increasing melt viscosity. The higher viscosity reduces the mobility and diffusivity of alkali ions, particularly K^+, which are essential for leucite nucleation. As a result, the nucleation rate of leucite is suppressed, and crystallization is shifted to higher temperatures. Under such conditions, crystallization occurs through a limited number of nuclei, which promotes enhanced crystal growth at elevated temperatures rather than uniform nucleation. This growth-dominated crystallization mechanism leads to the formation of coarser leucite crystals and an inhomogeneous microstructure. The resulting microstructural heterogeneity, characterized by uneven crystal distribution and residual glassy regions, adversely affects densification and mechanical performance. Similar diffusion-controlled crystallization behavior has been reported for alumina-rich aluminosilicate glass-ceramics in previous studies.

3.5. Mechanical Properties

According to the Vickers hardness and flexural strength data presented in Table 3, sample A18, which contains the lowest alumina content, exhibits the highest hardness and flexural strength. This superior mechanical performance can be attributed to its higher relative density (Table 3), greater amount of leucite phase (Figure 4e, where the intensity of the leucite diffraction peak is highest for A18 and lowest for A26), more homogeneous microstructure (Figure 5 and Ref (Kumar et al., 2016).), and finer crystalline grain size (Zhang et al., 2008).

The flexural strength values obtained in the present study (approximately 38–50 MPa) are consistent with those reported for leucite-based dental glass-ceramics fabricated via conventional melting–quenching routes. For instance, Cattell et al. and Denry and Kelly reported flexural strength values in the range of 35–60 MPa, depending on leucite content and heat-treatment conditions. The decrease in strength observed at higher alumina contents in the present study agrees with previous findings indicating that excessive alumina adversely affects densification and microstructural uniformity, ultimately leading to reduced mechanical performance (Cattell et al., 2020; Denry & Holloway, 2010; Kelly, 2004). The lower flexural strength observed in sample A22 can be explained by the presence of coarser crystalline grains and higher porosity, which act as stress concentrators and promote crack initiation. Similar relationships between microstructure and mechanical strength have been reported by Morena et al. and Caesar et al., who demonstrated a direct correlation between porosity, leucite morphology, and the flexural strength of dental porcelains (Morena et al., 1986). It should also be noted that the hardness and strength of the leucite crystalline phase, acting as a reinforcing phase, are higher than those of the glassy matrix and other potassium-based aluminosilicates (Kumar et al., 2016; Zhang et al., 2008; 橋本忍 et al., 2005). Finally, the lower hardness and flexural strength of sample A22 compared with A26 can be attributed to the presence of potassium-rich feldspar phases in A22, which negatively influence microstructural uniformity and mechanical performance. Microstructural heterogeneity was further assessed based on the grain size distribution obtained from image analysis. Although the average grain size increased from A18 to A22 and A26, a broader grain size distribution was observed for samples with higher alumina content, particularly A22. This wider distribution, characterized by the coexistence of fine and coarse leucite crystals, indicates increased microstructural heterogeneity. In contrast, sample A18 exhibited a narrower grain size distribution and a more uniform dispersion of fine leucite crystals. The increased microstructural heterogeneity had a direct impact on the mechanical properties. Samples with broader grain size distributions and higher heterogeneity, especially A22, exhibited lower flexural strength and hardness due to the presence of coarse grains and residual porosity, which act as stress concentrators and promote crack initiation.

Conversely, the more homogeneous microstructure of A18 resulted in improved load distribution, enhanced crack deflection, and superior mechanical performance. Similar relationships between grain size distribution, microstructural homogeneity, and mechanical properties have been reported for leucite-based dental glass-ceramics in the literature.

4. CONCLUSION(S)

In this study, the effect of alumina content on the microstructure and properties of dental leucite-based glass-ceramics was systematically investigated. Glass compositions containing 18–26 wt.% $Al(OH)_3$ were prepared via melting–quenching and subsequently heat treated in the temperature range of 700–1000 °C. The main findings can be summarized as follows: XRD analysis revealed that leucite crystallization occurred at higher heat-treatment temperatures in samples with higher alumina content, indicating a delay in crystallization. At a given heat-treatment temperature, samples with higher alumina content exhibited significantly lower intensities of leucite diffraction peaks, further confirming suppressed crystallization kinetics. Compositions with lower alumina content showed higher melt fluidity during the melting stage and achieved greater densification and more pronounced crystallization after heat treatment. SEM observations demonstrated that increasing alumina content led to coarser crystalline features and reduced microstructural homogeneity. Mechanical properties, including Vickers hardness and flexural strength, were highest for the sample with the lowest alumina content (A18). The optimal heat-treatment temperature for the composition containing 18 wt.% $Al(OH)_3$ was determined to be 950 °C. Overall, increasing alumina content beyond the stoichiometric requirement for leucite formation reduces microstructural homogeneity, relative density, and mechanical performance of leucite-based dental glass-ceramics, although it may enhance chemical durability. The optimized composition (A18) therefore represents a promising candidate for restorative dental applications, offering a favorable balance between mechanical strength and aesthetic compatibility.

DATA AVALLABLITY

All data generated or analyzed during this study are included within this published article.

ACKNOWLEDGEMENTS

We would like to thank the department of mining & matallurgical engineering -Yazd University, for providing financial and equipment support for this research.

REFERENCES

1. Al-Sanabani, F. A., Madfa, A. A., & Al-Qudaimi, N. H. (2014). Alumina ceramic for dental applications: A review article. *Am. J. Mater. Res*, *1*(1), 26-34. https://www.researchgate.net/publication/261426535
2. Aydınoğlu, A., & Yoruç, A. B. H. (2017). Effects of silane-modified fillers on properties of dental composite resin. *Materials Science and Engineering: C*, *79*, 382-389. https://doi.org/10.1016/j.msec.2017.04.151
3. Baino, F., & Verné, E. (2017). Production and characterization of glass-ceramic materials for potential use in dental applications: Thermal and mechanical properties, microstructure, and in vitro bioactivity. *Applied Sciences*, *7*(12), 1330. https://doi.org/10.3390/app7121330
4. Cattell, M. J., Patzig, C., Bissasu, S., Tsoutsos, A., & Karpukhina, N. (2020). Nucleation efficacy and flexural strength of novel leucite glass-ceramics. *Dental Materials*, *36*(5), 592-602. https://doi.org/10.1016/j.dental.2020.03.017
5. Chen, J., Qin, J., Lu, L., Li, H., Miao, X., Niu, L., Liu, H., Zhou, G., Yao, C., & Yuan, X. (2019). Study on laser-stricken damage to alumina ceramic layer of different surface roughness. *Results in Physics*, *15*, 102723. https://doi.org/10.1016/j.rinp.2019.102723
6. Chen, Q.-Z., Li, Y., Jin, L.-Y., Quinn, J. M., & Komesaroff, P. A. (2010). A new sol–gel process for producing Na2O-containing bioactive glass ceramics. *Acta biomaterialia*, *6*(10), 4143-4153. https://doi.org/10.1016/j.actbio.2010.04.022
7. Denry, I., & Holloway, J. A. (2010). Ceramics for dental applications: a review. *Materials*, *3*(1), 351-368. https://doi.org/10.3390/ma3010351
8. Denry, I., & Kelly, J. R. (2008). State of the art of zirconia for dental applications. *Dental Materials*, *24*(3), 299-307. https://doi.org/10.1016/j.dental.2007.05.007
9. El-Meliegy, E., & Van Noort, R. (2011). *Glasses and glass ceramics for medical applications*. Springer science & business media, https://www.google.com/books/edition/Glasses_and_Glass_Ceramics_for_Medical_A/SOlLoYcf3_UC?hl=en
10. Fu, L., Engqvist, H., & Xia, W. (2020). Glass–ceramics in dentistry: A review. *Materials*, *13*(5), 1049. https://doi.org/10.3390/ma13051049
11. Gómez Tamayo, J., Rueda Arango, A. O., & Ossa Henao, E. A. (2020). Improving the mechanical properties of commercial feldspathic dental porcelain by addition of Alumina-Zirconia. *Revista Facultad de Ingeniería Universidad de Antioquia*(94), 67-76. http://doi.org/10.17533/udea.redin.n91a11
12. Höland, W., & Beall, G. H. (2012). *Glass-ceramic technology 346*. Wiley Online Library. https://onlinelibrary.wiley.com/doi/book/10.1002/9781118265987
13. Kelly, J. R. (2004). Dental ceramics: current thinking and trends. *Dental Clinics*, *48*(2), 513-530. https://doi.org/10.1016/j.cden.2004.01.003
14. Kelly, J. R., Nishimura, I., & Campbell, S. D. (1996). Ceramics in dentistry: historical roots and current perspectives. *The Journal of prosthetic dentistry*, *75*(1), 18-32. https://doi.org/10.1016/S0022-3913(96)90413-8
15. Kumar, P., Srivastava, A., Kumar, V., Singh, H., Sharma, S., Kumar, P., & Singh, V. (2015). Role of CaF2 on mechanochemically synthesized leucite as dental veneering glass ceramics. *Advances in Applied Ceramics*, *114*(2), 107-113. https://doi.org/10.1179/1743676114Y.0000000208
16. Kumar, P. H., Singh, V. K., Kumar, P., Yadav, G., & Chaturvedi, R. (2016). Effect of Al2O3 on leucite based bioactive glass ceramic composite for dental veneering. *Ceramics International*, *42*(2), 3591-3597. https://doi.org/10.1016/j.ceramint.2015.11.022

17. Kumar, P. H., Singh, V. K., Srivastava, A., Hira, S. K., Kumar, P., & Manna, P. P. (2015). Mechanochemically synthesized leucite based bioactive glass ceramic composite for dental veneering. *Ceramics International*, *41*(9), 11161-11168. https://doi.org/10.1179/1743676114Y.0000000208

18. Mackert Jr, J., Twiggs, S., Russell, C., & Williams, A. (2001). Evidence of a critical leucite particle size for microcracking in dental porcelains. *Journal of dental research*, *80*(6), 1574-1579. https://doi.org/10.1177/00220345010800061901

19. Montazerian, M., Baino, F., Fiume, E., Migneco, C., Alaghmandfard, A., Sedighi, O., DeCeanne, A. V., Wilkinson, C. J., & Mauro, J. C. (2023). Glass-ceramics in dentistry: Fundamentals, technologies, experimental techniques, applications, and open issues. *Progress in Materials Science*, *132*, 101023. https://doi.org/10.1016/j.pmatsci.2022.101023

20. Montazerian, M., & Zanotto, E. D. (2017). Bioactive and inert dental glass-ceramics. *Journal of Biomedical Materials Research Part A*, *105*(2), 619-639. https://doi.org/10.1002/jbm.a.35923

21. Morena, R., Beaudreau, G., Lockwood, P., Evans, A., & Fairhurst, C. (1986). Fatigue of dental ceramics in a simulated oral environment. *Journal of dental research*, *65*(7), 993-997. https://doi.org/10.1177/00220345860650071901

22. Mrázová, M., & Klouzkova, A. (2009). Leucite porcelain fused to metals for dental restoration. *Ceramics-Silikáty*, *53*(3), 225-230. https://www.irsm.cas.cz/materialy/cs_content/2009/Mrazova_CS_2009_0000.pdf

23. Novembre, D., Gimeno, D., & Poe, B. (2019). Synthesis and characterization of leucite using a diatomite precursor. *Scientific Reports*, *9*(1), 10051. https://doi.org/10.1038/s41598-019-46569-y

24. Salimkhani, H., Asghari Fesaghandis, E., Salimkhani, S., Abdolalipour, B., Motei Dizaji, A., Joodi, T., & Bordbar-Khiabani, A. (2019). In situ synthesis of leucite-based feldspathic dental porcelain with minor kalsilite and Fe2O3 impurities. *International Journal of Applied Ceramic Technology*, *16*(2), 552-561. https://doi.org/10.1111/ijac.13142

25. Srichumpong, T., Angkulpipat, S., Prasertwong, S., Thongpun, N., Teanchai, C., Veronesi, P., Suputtamongkol, K., Leonelli, C., Heness, G., & Chaysuwan, D. (2020). Effect of the crystallisation time and metal oxide pigments on translucency and the mechanical and physical properties of mica glass-ceramics. *Journal of Non-Crystalline Solids*, *528*, 119730. https://doi.org/10.1016/j.jnoncrysol.2019.119730

26. Stábile, F. M., & Volzone, C. (2014). Bioactivity of leucite containing glass-ceramics using natural raw materials. *Materials Research*, *17*, 1031-1038. https://doi.org/10.1590/1516-1439.267014

27. Sui, L. N., Yu, L. Y., & Dong, L. F. (2011). Study on Properties of Leucite for Dental Porcelain Compositions. *Applied Mechanics and Materials*, *66*, 1522-1527. https://doi.org/10.4028/www.scientific.net/AMM.66-68.1522

28. Xie, N., Bell, J. L., & Kriven, W. M. (2010). Fabrication of structural leucite glass–ceramics from potassium-based geopolymer precursors. *Journal of the American Ceramic Society*, *93*(9), 2644-2649. https://doi.org/10.1111/j.1551-2916.2010.03794.x

29. Yoon, C. K., Rasmussen, S. T., O'Brien, W. J., & Tien, T.-Y. (1994). Properties of leucite-glass composites prepared by a coprecipitation process. *Journal of materials research*, *9*(9), 2285-2289. https://doi.org/10.1557/JMR.1994.2285

30. Zhang, Y.-R., Du, W., Zhou, X.-D., & Yu, H.-Y. (2014). Review of research on the mechanical properties of the human tooth. *International journal of oral science*, *6*(2), 61-69. https://doi.org/10.1038/ijos.2014.21

31. Zhang, Y., Rao, P., Lü, M., & Wu, J. (2008). Mechanical properties of dental porcelain with different leucite particle sizes. *Journal of the American Ceramic Society*, *91*(2), 527-534. https://doi.org/10.1111/j.1551-2916.2007.02179.x

32. Shinobu H., Fumiharu S., Sawao H., Hideo A., Koichiro F. (2005). Fabrication and mechanical properties of sintered leucite body. *Journal of the Ceramic Society of Japan*, *113*(1319), 488-490. https://doi.org/10.2109/jcersj.113.488